scientific reports

Check for updates

OPEN

Characterization of ovine abortion in Uruguay reveals extensive non-clonal diversity and multiple evolutionary origins of *Toxoplasma gondii*

Leandro Tana-Hernandez[1], Pablo Fresia[2], Andrés M. Cabrera[3], Alejandra Valentin[1], Matías Dorsch[4], Sergio Fierro[5], Federico Giannitti[4], Luisa Berná[1,6,7]✉ & María E. Francia[1,3]✉

Toxoplasma gondii **is a major cause of reproductive losses in farm animals worldwide, with sheep being a particularly sensitive species. Yet, the diversity and biological characteristics of strains associated with ovine abortion remain incompletely understood in many regions, including South America whereby genetic diversity is known to be high. In this study, we investigated the genetic diversity of *T. gondii* associated with ovine abortion in Uruguay through genotyping and phylogenetic analyses of samples obtained from abortion cases. To place the observed diversity in a broader epidemiological context, ovine data were compared with previously reported genotypes circulating in humans locally. In addition, two novel strains were isolated from independent ovine abortion cases and subjected to determination of their infectivity both in vitro and in vivo, as well as to whole-genome sequencing. Integrated analyses revealed that the isolates represent previously undescribed genotypes and display marked differences in virulence-associated traits. Genomic analysis identified variation in loci previously linked to parasite virulence, including differences in ROP5 copy number. Together, our results provide new insight into the diversity of *T. gondii* associated with ovine abortion in Uruguay and expand current knowledge of the biological and genomic features of strains circulating in this species.**

Keywords *Toxoplasma gondii*, Sheep abortion, *In-silico* RFLP, Genotyping, Genome sequencing, Virulence, Gene copy number variation

Toxoplasma gondii is a zoonotic protozoan parasite of worldwide distribution, which showcases its ability to infect most warm-blooded vertebrates, including terrestrial and marine mammals, and birds[1,2]. Its success as a parasite is partially owed to its multiple life stages, and transmission routes. Within the intermediate hosts, *T. gondii* can exist as a fast replicating tachyzoite capable of invading and destroying virtually any nucleated cell, causing an acute infection. It can then persist chronically in a latent encysted form known as bradyzoite[3]. Cats and other felids serve as definitive hosts sustaining parasite sexual stages, which enables sexual recombination, and the release of infectious oocysts into the environment[4,5]. Transmission occurs through ingestion of food contaminated with sporulated oocysts or raw, undercooked meat that contains bradyzoite tissue cysts[6]. Notably, *T. gondii* can also be transmitted transplacentally, which leads to congenital infection and/or abortion[7]. Though the impact of transplacental transmission of *T. gondii* on human abortion has not been systematically quantified, it is well established that sheep, goat and pigs, are particularly sensitive to *T. gondii* infection during pregnancy. *T. gondii* is in fact a leading cause of reproductive loss in these animals[8].

[1]Laboratory of Apicomplexan Biology, Institut Pasteur de Montevideo, Montevideo, Uruguay. [2]Unidad Mixta Pasteur + INIA (UMPI), Institut Pasteur de Montevideo, Montevideo, Uruguay. [3]Unidad Académica de Parasitología y Micología, Facultad de Medicina, Instituto de Higiene, Universidad de la República, Montevideo, Uruguay. [4]Plataforma de Investigación en Salud Animal, Instituto Nacional de Investigación Agropecuaria (INIA), Estación Experimental La Estanzuela, Colonia, Uruguay. [5]Secretariado Uruguayo de la Lana, Montevideo, Uruguay. [6]Bioinformatic Unit, Institut Pasteur de Montevideo, Montevideo, Uruguay. [7]Laboratorio de Genómica Evolutiva, Facultad de Ciencias, Universidad de la República, Montevideo, Uruguay. ✉email: lberna@pasteur.edu.uy; mfrancia@pasteur.edu.uy

The population genetic structure of *T. gondii* both in North America and Europe is primarily composed of clonal lineages originally termed "typical." These genetic types, named I through III, differ in virulence and species distribution. Type I strains are the least frequent in nature and the most virulent in murine models. In contrast, type II strains are more common, display intermediate virulence in the mouse model[9,10], and are the predominant type found in sheep and other livestock[11,12]. On the other hand, it is well established that in South America, the predominant genetic types are combinations of alleles found in strains of types I-III[13]. These strains are named "non-clonal". In addition, South American strains include novel alleles distinct from those found in Types I to III; these strains are known as "non-archetypal". A handful of in-depth characterized strains display phenotypic traits of exacerbated virulence, increased tendency to encyst, and resistance to the drugs used in clinical settings[14–16]. However, the relationship between non-clonal and non-archetypal genotypes and phenotype is yet to be fully clarified. Most research aiming to uncover the molecular underpinnings of phenotypes has relied on laboratory-adapted strains, some of which have lost key virulence-related traits, such as the ability to form brain cysts in mice. In addition, studies designed to systematically compare strains often lack harmonized methodologies[17]. Consequently, there is a significant knowledge gap in the understanding of the impact of naturally occurring variability on clinically relevant phenotypes.

Previous studies have identified gene copy number variations of the secreted pseudo kinase ROP5 to play a pivotal role in virulence. The higher the number of ROP5 genes, the greater the virulence of the strain[18,19]. However, this was determined in a laboratory strain and its relevance to strains circulating in the wild remains unknown.

Previous work by our group and others have shown that *T. gondii* is a major cause of ovine abortion in Uruguay[20–23], mirroring the situation of other South American countries[24]. Pioneering work from Freyre and colleagues isolated a highly virulent non-clonal *T. gondii* strain from a sheep aborted fetus in Uruguay[22,25]. This particular strain, known as "CASTELLS", belongs to clade E clustering together with other non-archetypal isolates[15,26]. However, despite the recognized impact of *T. gondii* on ovine reproductive health, the diversity of parasite genotypes associated with abortion in Uruguay and their biological characteristics remain poorly understood. In this study, we aimed to characterize the genetic diversity of *T. gondii* detected in ovine abortion cases and to place these findings within the broader context of parasite diversity circulating in the region. To this end, we performed genotyping and phylogenetic analyses of samples obtained from abortion cases and compared these data with genotypes previously reported in humans. In addition, we isolated parasite strains from independent ovine abortion cases and performed genomic characterization of these isolates, as well as in vitro and in vivo characterization of their virulence. Although these isolates were not derived from the same cohort analyzed in the genotyping survey, they provide an opportunity to explore biological and genomic features of parasites associated with abortion in this species. By integrating epidemiological, experimental, and genomic approaches, this work provides a broader view of the diversity and biological properties of *T. gondii* in ovine abortions.

Materials and methods

Study samples and DNA extraction

Placental and fetal tissue samples were derived from 58 sheep abortions obtained from sheep flocks residing in different locations within Uruguay (as indicated in **Supplementary Fig. 1**). Samples were voluntarily rendered by sheep owners and first sent to the "Plataforma de Investigación en Salud Animal, Estación Experimental INIA La Estanzuela" in Colonia, Uruguay for diagnosis. Here, *T. gondii* infection and associated disease was confirmed by histopathology, and positive parasite DNA detection by PCR as reported previously[20]. All samples were reanalyzed for *T. gondii* DNA detection as described below prior to proceeding with the in silico RFLP analysis.

Genomic DNA was extracted from tissues or cell cultures using the Quick-DNA Tissue/Insect MiniPrep Kit (Zymo Research, D6016) following the manufacturer's instructions and stored at − 20 °C–4 °C until further analysis. *T. gondii* DNA was detected by PCR using specific primers (**Supplementary Table 1**) and MangoMix master mix (Meridian Biosciences, BIO-25033), as previously described[27,28].

In silico PCR-RFLP genotyping and phylogenetic

Strain genotype determination (also referred to as "typing") was carried out by in *silico* analyses of genetic markers as previously described by[29]. Amplification of twelve markers (SAG1, 5'–3' SAG2, Alta SAG2, SAG3, BTUB, GRA6, c22-8, c-29-2, L358, PK1 and Apico) was carried out by nested PCR as previously described in[16] We were consistently unable to amplify the "Apico" marker. Following successful amplification of markers, Sanger sequencing of amplicons was performed (Macrogen Inc., South Korea). Detection of polymorphic profiles was carried out as described by Castro and collaborators[30] and used as in[31] without modifications. Genotype assignments are detailed in Supplementary Table 2. All marker sequences were deposited in GenBank (accession numbers in Supplementary Table 3).

Chromatograms were visually inspected, and ambiguous base calls were manually curated. Sequences were aligned using MAFFT[32], and alignment confidence was assessed with rGUIDANCE[33]. Confidence scores were incorporated as weights in downstream analyses. Maximum-likelihood phylogenies were inferred with RAxML[34] under the GTRCAT model. A Neighbor-Joining tree based on TN93 distances was used as the starting topology. Gene-partitioned analyses were specified using a partition file, and node support was evaluated with 100 rapid bootstrap replicates.

Strain isolation and cell culture

Strain isolation was carried out as described in[35] without modifications. In short, placenta tissue from a fetal loss case derived in the Department of Colonia in 2021 (TgUru2) and fetal brain tissue (TgUru1) from an aborted fetus from Florida were used. Tissues were homogenized in Phosphate-buffered saline (PBS) solution containing

antibiotics using a manual douncer. DNA was extracted from a fraction of the homogenate to determine by PCR whether the sample contained traces of *T. gondii* DNA, following the PCR-based DNA detection procedures described above. A maximum of 200 µl of PCR-positive homogenates were intraperitoneally injected into Interferon gamma knockout B6 mice. Animals were monitored daily for clinical signs. Symptomatic mice were euthanized, and brain tissue and peritoneal fluid were collected. *T. gondii* presence was confirmed by PCR and phase-contrast microscopy. Parasites were subsequently propagated in VERO cells cultured in DMEM supplemented with 10% fetal bovine serum and 1% penicillin/streptomycin at 37 °C in 5% CO_2.

In vitro invasion and growth assays

Intracellular growth and invasion assays were conducted following the procedures described in[36] with the following modifications; assays were performed by infecting confluent neonatal Human Dermal Fibroblasts (HDFn) cultured on 13 mm coverslips with 1000 parasites. Quantification was performed by determining the number of parasites per field (invasion) and the number of parasites per vacuole 24 h post-infection (growth). Parasites were visualized by immunofluorescence assays performed as previously described by[37], using an Olympus epifluorescence microscope and a 60x oil lens. All assays were conducted in triplicate, with the *T. gondii* PruΔKu80 strain serving as control, and 50 randomly selected fields were quantified for each experiment.

In vivo phenotypic characterization

To assess acute virulence, female BALB/c mice (6–8 weeks old $n = 4$ per group) were intraperitoneally infected with defined parasite doses suspended in PBS. Sterile PBS was used as negative control. Seroconversion was evaluated by Western blot (data not shown).

For brain cyst quantification, BALB/c mice were infected with 100 parasites of TgPruΔKu80 or TgUru2. Fifteen days post-infection, brains were collected and processed as previously described[38]. Briefly, tissues were homogenized using a Pellet Pestle, fixed with 3% formaldehyde, quenched with 0.1 mM glycine, and blocked/permeabilized overnight at 4 °C in blocking solution (3% BSA, 0.2% Triton X-100). Samples were stained with Fluorescein-conjugated DBA (Vector Laboratories, 1:500). Five microliters of each sample were placed on glass slides and coverslips in triplicate. Cyst counts were pursued using an Olympus IX81 epifluorescence microscope using a 40X objective. Statistical analysis was carried out using an unpaired Student's t-test in GraphPad.

Whole-genome sequencing and comparative genomic analyses

Whole-genome sequencing was performed using Oxford Nanopore Technologies (ONT) long reads and DNBseq short reads (BGI Genomics). ONT libraries were prepared using the Rapid Barcoding Kit (SQK-RBK004) from 400 ng genomic DNA and sequenced on a MinION Mk1C device with R9.4.1 flow cells. Base calling was performed with Guppy v3.0.3. Short reads were generated in paired-end mode (2×150 bp). Long reads were assembled de novo using Canu[39]. Apicoplast and mitochondrial contigs were identified by GC content and sequence similarity and removed. Contigs lacking homology to the *T. gondii* reference genome were inspected by BLASTn and discarded as contaminants. Assemblies were polished using Racon (long-read correction) followed by two rounds of Pilon[40] using short reads aligned with BWA-MEM[41] Final assemblies were scaffolded against the RHΔKu80 reference genome using ABACAS[42]. RNA-seq data (SRR23391969–SRR23391971) were aligned with HISAT2[43,44], transcripts assembled with StringTie[45], and gene models predicted using COMPANION[46], with *T. gondii* ME49 as reference.

Comparative genome analyses were conducted using nucmer (MUMmer[47], and structural variants were identified with Assemblytics[48]. Genomic synteny was visualized using Circos[49].

Copy number variation and ROP5 characterization

Copy number variation (CNV) was assessed for a curated set of 53 genes encoding rhoptry (ROP) and dense granule (GRA) effectors implicated in host invasion and immune modulation. Gene IDs were retrieved from ToxoDB and are listed in Supplementary Table 5. Homology searches were performed using BLASTn and BLASTp against the TgUru1 and TgUru2 assemblies to determine gene presence, absence, and relative copy number compared to the RH reference strain.

Given the differences observed in ROP5 copy number among the analyzed isolates, additional analyses were performed to characterize the ROP5 subtypes present in each genome. Predicted ROP5 peptide sequences from TgUru1 and TgUru2 were aligned together with all ROP5 protein sequences available in UniProt/TrEMBL at the time of analysis ($n = 52$; accession numbers listed in **Supplementary Table 8**).

Multiple sequence alignments were generated using MAFFT (--auto). Phylogenetic classification of ROP5 variants was performed using IQ-TREE2[50] under the GTR + F substitution model, with 1,000 ultrafast bootstrap replicates and 1,000 SH-aLRT replicates to assess node support. To further examine conserved features of the pseudokinase domain, a representative subset of ROP5 proteins was selected for detailed alignment. This subset included the following UniProt/TrEMBL accessions: I6YX69 (ROP5A), F2YGR7 (ROP5B), I6ZQR7 (ROP5C), F2YGS5, F2YGS7, F5XVD7, Q3YJR4, A0A125YQ30, F5XVD5, and F5XVD6, together with the eight ROP5 copies identified in TgUru1 and TgUru2. Alignments were generated with MAFFT (--auto) and manually inspected to evaluate conservation across key catalytic and structural motifs.

Phylogenetic analysis of strains

A dataset of 53 strains was analyzed, comprising TgUru1 and TgUru2, 46 hybrid isolates from the Americas described by[51], the previously reported Uruguayan strain CASTELLS, and the canonical laboratory reference strains TgME49, TgVEG, TgRH, and TgPRU. Public Illumina reads were retrieved from the NCBI SRA (**Supplementary Table 7**) and aligned to the RH reference genome (TgRH_pasteur, GCA_033216535.1[52] using BWA-MEM. Variant calling followed GATK Best Practices[53], and high-confidence SNPs and indels were retained

after hard filtering. A curated set of 100 single-copy nuclear genes (**Supplementary Table 6**) was extracted for phylogenetic inference. Gene sequences were reconstructed using FastaAlternateReferenceMaker, concatenated, aligned with MAFFT, and analyzed with IQ-TREE2 under the GTR + F model with 1,000 bootstrap and SH-aLRT replicates. Trees were visualized using iTOL[54].

Use of animals for experimentation

All protocols pertaining to the use of experimental animals were pre-approved by the Institutional Ethics Committee of the Institut Pasteur de Montevideo (CEUA No. 019–19 and 023 – 22). Animals were bred at the Laboratory Animal Biotechnology Unit of the Institut Pasteur de Montevideo under specific pathogen-free conditions in ventilated racks (IVC, 1285 L, Tecniplast, Milan, Italy), housed in pathogen-free specific facilities and subjected to daily monitoring.

Humanitarian criteria for animal endpoints were strictly followed in accordance with the established norms. Euthanasia was performed by first inducing deep anesthesia through intraperitoneal administration of a ketamine/xylazine combination. Mice were anesthetized by intraperitoneal injection of a freshly prepared ketamine–xylazine 2% solution, administered at a volume of 10 mL/kg, corresponding to doses of 110 mg/kg ketamine (phs® Pharmaservice Montevideo-Uruguay) and 13 mg/kg xylazine (Laboratorios Microsules Uruguay S.A.). Anesthetic depth was verified by the absence of motor responses to nociceptive stimulation of the forelimbs and hindlimbs, after which cervical dislocation was carried out as the physical method of euthanasia. All experiments were carried out in accordance with relevant guidelines outlined in the animal experimentation protocol, abiding by the national animal protection law (No. 18.611) and the ARRIVE guidelines[55].

Results

The study consisted of two complementary components: (i) genotyping and phylogenetic analysis of *T. gondii* detected in ovine abortion cases, and (ii) biological and genomic characterization of isolates obtained from independent abortion events.

Sixteen sheep samples, labeled TgShUru1-16, exhibiting a positive PCR result for *T. gondii* DNA detection were subjected to amplification of 11 conventional genotyping markers. Amplicons were sequenced, and their restriction patterns were analyzed in silico using established enzymes (Fig. 1A). All 16 samples displayed amplification of at least one typing marker with most samples amplifying Gra6 (14/16) and/or Btub (10/16). PCR amplification success across the remaining markers (SAG1, SAG2, 5'–3' SAG2, SAG3, c29-2, c22-8, L358, and PK1) was variable. Apico could not be amplified for any of the samples.

Among all characterized samples, a limited number displayed amplification patterns consistent exclusively with clonal alleles. Samples TgShUru1, TgShUru2, and TgShUru13 exhibited only type I alleles; however, in these cases, only one or two loci could be resolved, indicating incomplete and potentially biased genotyping. Three samples exhibited all amplified loci of clonal origin; TgShUru5 boasts virtually all Type III alleles; TgShUru3 and TgShUru7 display Type II alleles. However, in these cases a final genotype could not be called as a number of alleles – which could potentially alter the genotype assignment of these samples – could not be amplified. In addition, 8 samples (50%) showed amplification of mixed clonal alleles, indicating the presence of non-clonal hybrid genotypes (Fig. 1B). In most cases, these corresponded to a mixture of type I and type II (TgShUru6, 10, 11, 14, and 16). However, two samples also showed a mixture of type II and III (TgShUru4 and 9), while one sample displayed a mixture of all three genotypes (TgShUru16). Finally, two samples (TgShUru8 and 12) displayed amplification of non-clonal, previously unreported, alleles for C22-8 and L358, respectively, and were classified as "unreported" (**Supplementary Fig. 2 A and B**).

TgShUru10 and 16 resulted in the greatest number of amplified loci (Fig. 1A), which allowed us to compare them with reported genotypes in ToxoDB. The genotype detected in sample 10 did not coincide with previously reported genotypes. However, the genotype detected for TgShUru16 matched a previously reported genotype found in samples TgCKGa04 and TgSKMs3. The latter two were found in DNA from a *T. gondii* infected chicken in Guatemala, and a striped skunk in the USA, respectively. No identifying genotype number has been assigned to these samples. Remarkably, despite poor amplification in many samples, 8 distinct genotypes could be unequivocally distinguished among the 16 analyzed samples.

To explore how the genetic diversity differed among strains causing abortion in sheep, we performed comparative analyses using the complete sequences of amplified alleles (Fig. 1C). By incorporating polymorphisms beyond restriction sites, this approach improved the resolution of strain variability and enabled comparisons with both archetypal reference strains and publicly available non-archetypal regional sequences. Several ovine abortion-derived samples (TgShUru3, 11, 14, 10, 12, 15, 1, 16, 6, 13 and 2) clustered within a major clade containing type I reference strains such as TgRH and TgGT1, together with numerous non-archetypal strains from the region. In contrast, a subset of samples (TgShUru7, 9, 4, 5 and 8) was positioned closer to type II and III reference strains, including TgME49 and TgVEG, and showed proximity to a previous Uruguayan isolate CASTELLS[21]. These patterns highlight the coexistence of multiple evolutionary lineages within *T. gondii* populations associated with ovine abortion.

To assess the relationship between ovine and human infections, we incorporated 32 genotypes previously identified in humans[31]. Human-derived genotypes were interspersed among ovine samples, supporting the absence of host-specific clustering and suggesting shared transmission dynamics.

While the genotyping analyses described above provide insight into the diversity of *T. gondii* associated with ovine abortion, these data alone do not allow evaluation of the biological properties of circulating parasites. To directly explore this aspect, we pursued parasite isolates from abortion cases that were independent from the cohort analyzed in the genotyping survey described above. For this, we first recovered placental tissue from an ewe that had undergone a spontaneous abortion and from the brain of an additional aborted fetus. Tissue homogenate was inoculated into immunonaive mice and peritoneal fluid was collected, analyzed by PCR for

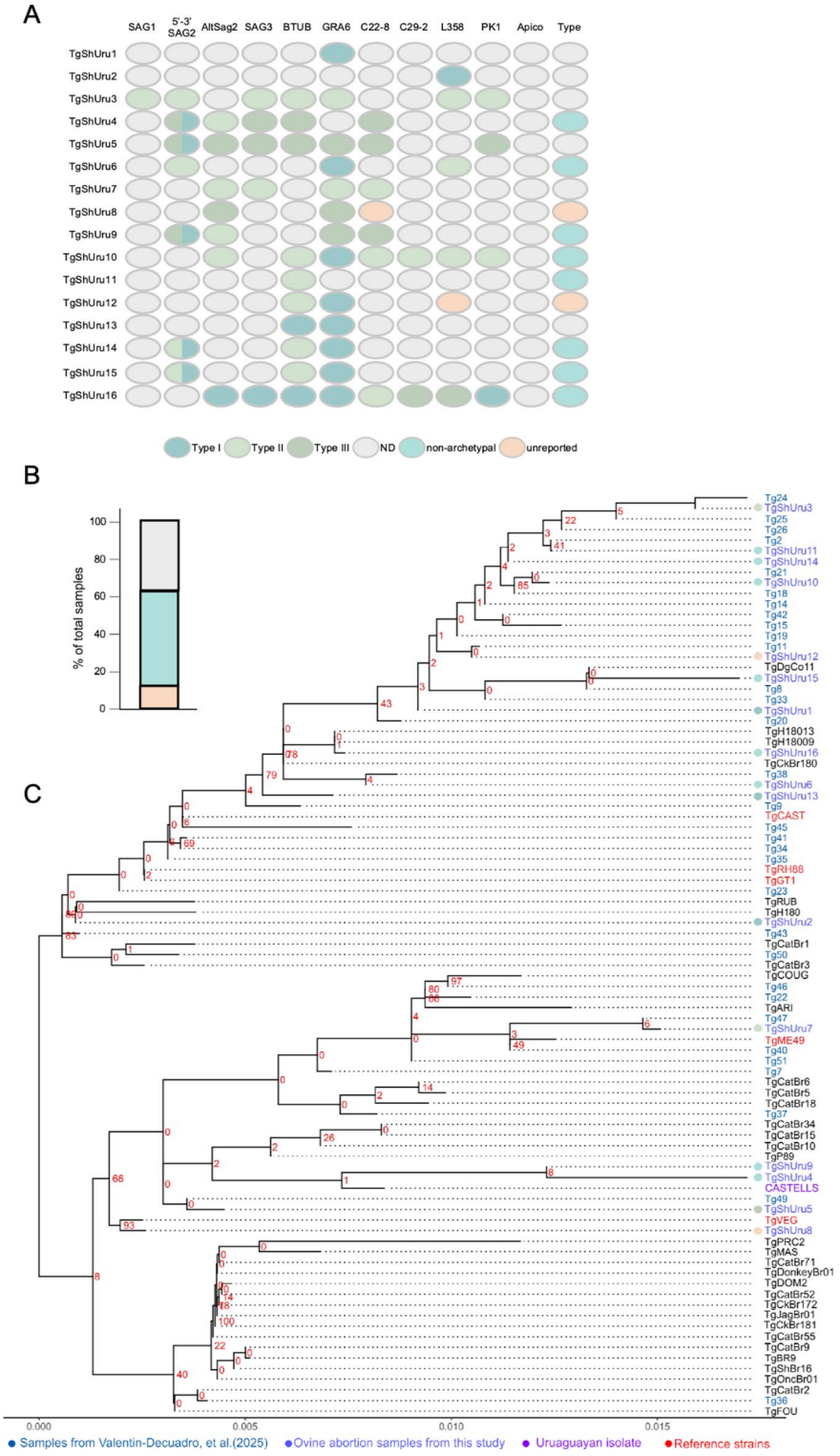

Fig. 1. *Genotyping of Toxoplasma gondii* strains causing abortion in sheep. (**A**) Schematic representation of the in silico RFLP analysis of 16 sheep abortion samples using the indicated markers. Genetic types were determined by analyzing the combination of genetic types obtained per marker, per sample. Results were color-coded as indicated. ND stands for *not determined*. Note that the "type" column summarizes genotype assignment per strain. (**B**) Quantification of genetic types found. The percentage of each assigned genotype in A was plotted. Results are color-coded as in A. (**C**) Phylogenetic analysis. A maximum likelihood tree reveals the presence of four phylogenetically distinct groups (1–4). Ovine abortion samples from this study are shown in blue. Genetically typed human samples from Uruguay are shown in teal and are labeled Tg1–51[31]. Reference strains are highlighted in red. Other strains are shown in black. A color-coded dot corresponding to the sample's genetic type, as identified in panel A, is displayed to the left of each sample for reference.

species confirmation, and transferred to cell culture (Figs. 2A **and C**, **and Supplementary Fig. 3**). Two isolates, named TgUru1 and TgUru2, were successfully established and expanded for further analyses. Genotyping indicated that these strains represent previously undescribed genotypes within the regional population structure of *T. gondii* (Fig. 2B). TgUru1 predominantly exhibits markers belonging to the type I lineage, in combination with a marker that does not fit into any of the clonal classifications and has not been reported previously (Supplementary Fig. 2C). TgUru2 predominantly displays markers belonging to type III and type I clonal lineages (Fig. 2B). When we incorporated these genotypes into an expanded phylogenetic framework, which included the human-derived genotypes and the rest of ovine samples shown in Fig. 1, TgUru1 and TgUru2 were placed in distinct regions of the tree, with TgUru1 closer to type I related sequences and TgUru2 nearer to type III associated lineages **(Supplementary Fig. 4)**. In addition, TgUru1 grouped closely with the ovine abortions sample TgShUru13. Comparison to the genotypes available in ToxoDB confirmed that they do not match any previously genotyped samples nor previously genotyped strains. Hence, TgUru1 and TgUru2 represent two novel non-clonal strains.

These isolates were subsequently characterized using in vitro assays, in vivo infections, and whole-genome sequencing in order to evaluate potential differences in virulence-associated traits and genomic features. First, we evaluated in vivo virulence in BALB/c mice. Clinical signs consistent with toxoplasmosis (hirsute hair, conjunctivitis, deterioration, and tachypnea) were readily observed in all mice infected with a single TgUru1 parasite as early as 7 days post infection, while mice infected with TgUru2 displayed a distinct disease evolution (Fig. 2D). All mice infected with 10^3 TgUru2 parasites remained asymptomatic and survived for the first four weeks post-infection. However, 50% of these mice later succumbed to infection by 32 dpi (Fig. 2D). Therefore, while TgUru1's lethal dose (LD100) is 1 parasite, TgUru2 displayed a comparable virulence rate to that displayed by the typical Type II strain Pru, with an LD75 of 10^3 parasites. However, TgUru2 triggered the onset of symptoms comparably later (Fig. 2B). To further explore TgUru2's infection kinetics, we assessed whether surviving mice were chronically infected. Indeed, we determined that the number of brain cysts generated by TgUru2 infected surviving mice was 4 times higher than those infected with equal doses of TgPru ($p = 0.0244$); while the brains of TgUru2 infected mice averaged 1543 cysts, TgPru infected mice averaged 381 cyst/brain (Fig. 2E).

To tackle the biology underlying these phenotypes we explored the strain's in vitro behavior. In addition to their detectable genetic differences, TgUru1 and TgUru2 differ dramatically in their in vitro growth patterns, with TgUru1 establishing high multiplicity of infection of the host cell cytosol and TgUru2 growing predominantly in clustered rosettes (Fig. 2C). We quantitated each strain's capacity to invade and proliferate within host cells.

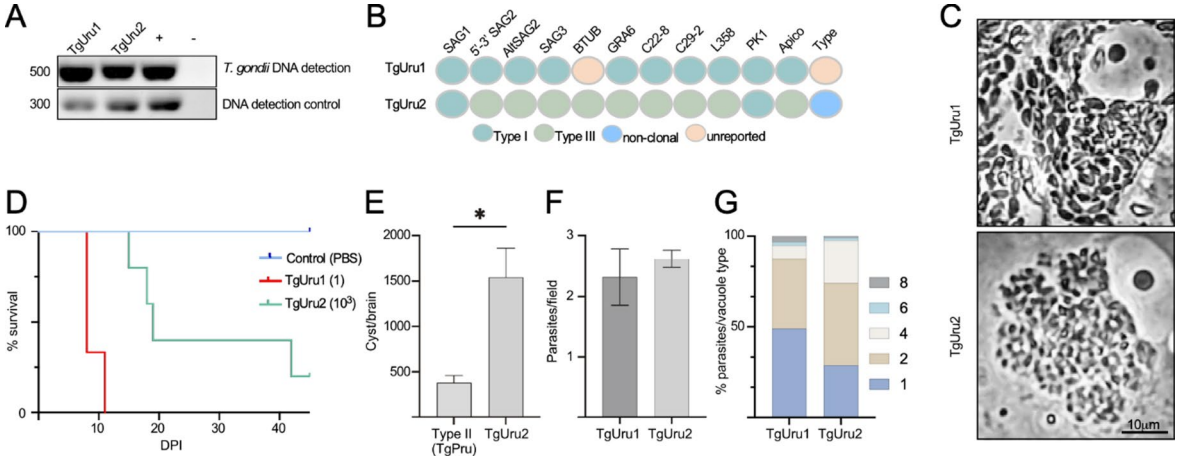

Fig. 2. Isolation of two novel non-clonal *Toxoplasma gondii* strains. (**A**) Isolate identity confirmation by specie-specific PCR. Detection of *T. gondii* DNA in peritoneal exudates from mice inoculated with homogenates of infected tissue enabled the establishment of two independent isolates named TgUru1 and TgUru2. + denotes positive DNA control. – denotes negative (no DNA) amplification control. Please note that the complete gel picture is included in Supplementary Fig. 2B. (**B**) Schematic representation of the in silico RFLP genotype determination of TgUru1 and TgUru2. PCR-RFLP genotyping revealed that both isolates are previously unreported non-clonal strains. TgUru1 carries predominantly type I alleles and some unclassified variants, whereas TgUru2 displays a mosaic of type III and type I alleles. No matching genotypes were found in ToxoDB. Results were color-coded as indicated. Note that the "type" column summarizes genotype assignment for each strain. (**C**) In vitro phenotype observation. TgUru1 presents fast and disseminated in vitro growth, while TgUru2 forms densely packed vacuoles. Scale bar represents 10 µm. (**D**) In vivo virulence determination. BALB/c (4 animals per condition) were inoculated with the indicated doses of TgUru1 and TgUru2, and with PBS as control. (**E**) Chronic infection cyst burden quantification. Surviving TgUru2 infected mice developed a markedly higher cyst load than animals infected with type II strain (TgPRU, mean 1543 vs. 381 cysts/brain; $p = 0.0244$). (**F**) Quantification of Invasion per strain. Both strains invaded host cells at comparable rates, as quantified by vacuole counts at 24 h postinfection. (**G**) Quantification of Early intracellular growth. TgUru1 more frequently accumulated in parasite vacuoles of 8, while TgUru2 parasite vacuoles consisted more often of 2–4 parasites, consistent with slower intracellular replication.

For this, equal numbers of TgUru1 and TgUru2 were allowed to invade host cells, subsequently grow for 24 h. The number of vacuoles per field of view was considered as a *proxy* for the number of invading parasites per strain, while the number of parasites per vacuole was considered a *proxy* for their intracellular replication rate. On average, we found that TgUru1 and TgUru2 exhibited similar invasion rates with no significant differences between the two (Fig. 2F). However, TgUru2 exhibited approximately half the number of vacuoles containing 8 parasites compared to TgUru1, with a concomitant increase in the proportion of vacuoles containing 2 and 4 parasites (Fig. 2G), suggesting that although both strains invade their host cells at comparable rates, once inside the cell, TgUru2's growth lags.

To investigate the genomic basis of the phenotypes observed in our isolates, we analyzed the structure, variability, and evolutionary relationships of the Uruguayan strains. Both genomes were sequenced using a combination of Oxford Nanopore Technologies long reads and DNBseq short reads, enabling high-contiguity assemblies and accurate polishing. Using publicly available RNA-seq datasets, we generated *de novo* gene annotations for each genome. Summary statistics for the assembled genomes and their corresponding annotations are presented in **Supplementary Table 4**.

Comparative analyses revealed that the overall genomic structure of TgUru1 and TgUru2 closely resembled that of the TgRH reference assembly previously generated by our group, with no major structural rearrangements detected (Fig. 3A and **Supplementary Fig. 5**). Given this structural conservation, we scaffolded both genomes onto the RH reference using ABACAS, recovering 13 chromosomes with lengths and composition comparable to the reference (Fig. 3A).

To quantify genetic divergence, we identified SNPs and indels in each genome relative to representative strains of the three classical lineages—type I (TgRH), type II (TgME49), and type III (TgVEG). Consistent with its close relationship to type I, TgUru1 showed very few variants relative to TgRH (13,302), whereas TgUru2 displayed a markedly higher number of differences (422,318). In contrast, when compared to the type III strain VEG, TgUru1 accumulated substantially more variants (481,708 vs. 292,817 for TgUru2), reflecting TgUru2's closer relation to type III. Relative to the type II strain TgME49, TgUru1 and TgUru2 carried 544,472 and 554,941 variants, respectively, reflecting a similarly large genetic distance from type II. Taken together, these results suggest that TgUru2 is genetically closer to Type III, whereas TgUru1 shows greater affinity to type I, consistent with our initial in silico PCR-RFLP typing.

We next examined copy number variation in virulence-associated effector gene families using the long-read assemblies. We focused on genes encoding rhoptry and dense-granule proteins involved in host invasion and immune modulation, including the pseudokinases ROP5 and ROP18, as well as additional virulence-associated effectors (GRA24, BFD1, MIC2, GRA7, and GRA17, among others). While the virulent reference strain TgRH carries four copies of ROP5, TgUru1 displays five. Conversely, TgUru2 bears three copies of ROP5 (Fig. 3B).

ROP5 displays underlying variability, reportedly encompassed by three canonical ROP5 subtypes named A, B, and C. These subtypes have been shown to differ in functionality[56], and virulence has been shown to correlate not only with the number of copies[19], but also with the strain's ROP5/ROP18 combination[26]. We thus set out to determine the ROP5 subtypes present in each genome. For this, we performed a phylogenetic analysis including all ROP5 gene copies identified in TgUru1 and TgUru2 together with the 52 ROP5 protein sequences available in UniProt (Fig. 3C). The resulting phylogeny shows that both Uruguayan isolates harbor representatives of the three canonical ROP5 subtypes (A, B, and C). As expected, subtypes B and C grouped more closely to each other than to subtype A.

The tree also revealed substantial sequence diversity within the ROP5 family, extending beyond the three subtypes originally defined by[57] (Fig. 3C). In several cases, proteins annotated in UniProt as ROP5A, ROP5B, or ROP5C did not cluster with their expected subtype, and in some instances intermingled with other groups, indicating inconsistencies in subtype annotation and highlighting the complexity of the ROP5 paralogous family. This pattern was also evident in the pairwise amino acid identity matrix derived from the multiple sequence alignment (**Supplementary Fig. 6**), which clearly distinguished the canonical type A clade from the more closely related Type B/C variants. Overall amino acid identity across all sequences averaged 94.5%, reflecting substantial conservation within each subtype and moderate divergence between them (Fig. 3D).

Inspection of the full multiple sequence alignment (**Supplementary Fig. 7**) showed that most of the variability is concentrated in the C-terminal pseudokinase domain, between positions 330 and 545. A focused alignment of a representative subset of proteins confirmed this pattern and revealed specific substitutions and small indels in some TgUru1 and TgUru2 copies (Fig. 3D). Notably, although the subtype-defining polymorphic sites were clearly identifiable, copies assigned to the same subtype (A, B, or C) showed little or no variation within the important regions in the pseudokinase domain (IRGa6, HGR and DVS), except for a two-guanine deletion observed in the TgUru1_1 ROP5 copy.

Beyond ROP5, several effectors involved in immune regulation (including GRA15 and GRA12C) are present in both Uruguayan isolates but absent in RH, suggesting lineage-specific retention or expansion among South American strains. Conversely, genes such as GRA4 and AP2XI-4 are absent in TgUru2, which may reflect localized gene loss, differential pseudogenization, or assembly differences supported by long-read evidence.

Finally, to place the Uruguayan isolates in a broader evolutionary context, we performed a comparative phylogenomic analysis using 100 conserved protein-coding genes across 53 *T. gondii* strains (Fig. 4). This dataset included TgUru1 and TgUru2, 46 hybrid isolates from the Americas described by[51], the previously reported Uruguayan strain CASTELLS, and the canonical laboratory reference strains TgME49, TgVEG, TgRH and TgPRU. Phylogenetic reconstruction revealed that the three Uruguayan strains fall into distinct clades. CASTELLS, previously associated with highly virulent non-clonal lineages, clustered separately and showed resemblance to several non-clonal Brazilian strains, yet remained genetically distinct. TgUru1 grouped with TgRH type I, and other hybrid strains from the Americas and the USA, whereas TgUru2 clustered within a lineage III–associated clade containing strains from the Americas and Africa. TgUru2 showed the closest,

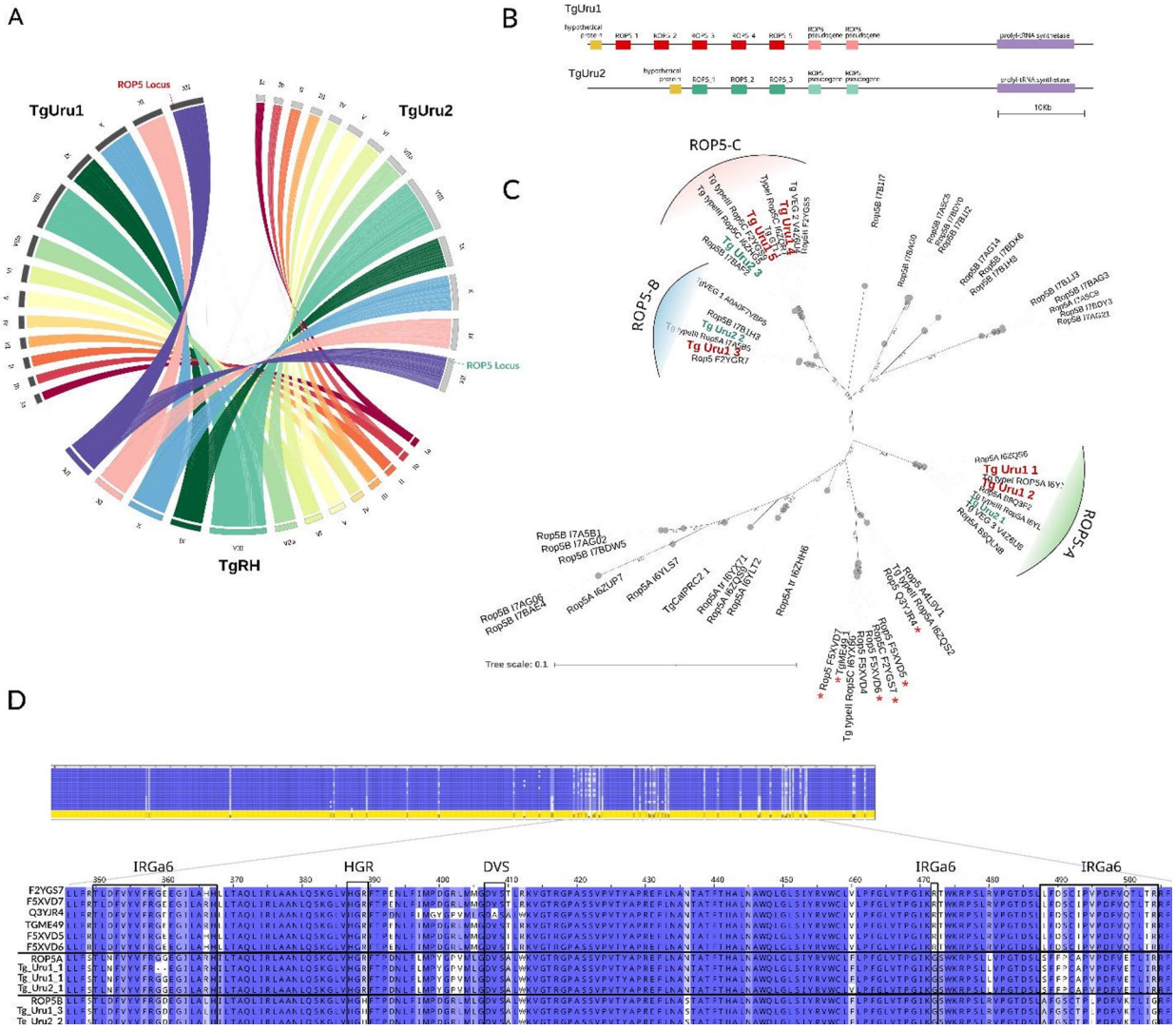

Fig. 3. Comparative genomic structure and ROP5 diversity in TgUru1 and TgUru2. (**A**) Genomic structure. Circos Plot of the genome alignment against RH reference assembly shows conserved chromosomal organization in both isolates TgUru1 and TgUru2, with no major structural rearrangements detected. Scaffolded assemblies recovered 13 chromosomes with lengths and composition comparable to that of TgRH. The ROP5 locus location is indicated. (**B**) Scaled representation of the ROP5 locus in TgUru1 and TgUru2. Copy number variation analysis revealed five ROP5 copies in TgUru1 and three in TgUru2. For reference, the RH strain contains four copies (not shown). (**C**) Phylogenetic reconstruction of ROP5 copies. Sequence comparisons among ROP5 copies present in TgUru1 and TgUru2, together with 52 reference ROP5 proteins from UniProt. Both isolates harbor representative members of the three canonical A/B/C subtypes (indicated on the tree). Asterisks denote the sequences selected for the subset alignment shown in panel (**D**). Focused alignment of a representative subset of ROP5 proteins. Alignment of selected ROP5 subtype members, shown with an asterisk in panel C, together with all copies from TgUru1 and TgUru2. The zoomed region highlights the C-terminal pseudokinase domain, where most sequence variants among ROP5 proteins are concentrated.

though still distant, relationship to TgVEG. None of the Uruguayan isolates clustered with TgME49 or TgPRU. Overall, these results indicate that Uruguayan *T. gondii* strains are highly divergent from one another, reflecting multiple, independent evolutionary origins.

Discussion

In this study, we combined epidemiological, experimental, and genomic approaches to investigate *Toxoplasma gondii* associated with ovine abortion in Uruguay. First, we characterized the diversity of parasite genotypes detected in abortion cases and compared these findings with genotypes previously reported in humans in the region. Second, we isolated parasite strains from independent abortion cases and examined their biological and genomic characteristics. Together, these complementary approaches provide new insight into the diversity of *T.*

Fig. 4. Genome-wide phylogeny of *Toxoplasma gondii* strains using 100 single-copy nuclear genes. Maximum-likelihood phylogeny inferred from 100 single-copy nuclear genes across 51 *Toxoplasma gondii* strains. Three Uruguayan isolates occupy distinct evolutionary positions and do not cluster with TgME49 or TgPRU, reflecting independent origins. CASTELLS groups with non-clonal Brazilian lineages, TgUru1 clusters with type I–related American hybrids, and TgUru2 falls within a lineage III–associated clade.

gondii circulating in this system and expand current understanding of strains associated with ovine reproductive disease.

Toxoplasmosis is considered one of the most globally distributed zoonotic diseases of both human and other animals[58,59]. It is estimated that one-third of the human and animal population has antibodies against *Toxoplasma*, indicating they are either chronically infected or have been exposed to the parasite[59,60]. Sheep are particularly sensitive to infection during pregnancy, and *T. gondii* is a well-recognized leading cause of abortion in this species worldwide[61]. In Uruguay, records from over 30 years ago identified *T. gondii* as a critically important infectious agent involved in gestational and neonatal losses in sheep[25]. A more recent study analyzing the causes of abortion in 100 ovine cases in Uruguay determined that 27% were still attributable to *T. gondii* infection[20].

Herein, we demonstrated that out of 16 abortion causing strains in sheep, 50% presented non-clonal genotypes with a combination of clonal strain loci and/or presence of previously unidentified RFLP patterns

(12.5%). Though the diversity of *T. gondii* genotypes present in sheep in Uruguay was previously unknown to this resolution; the genetic heterogeneity in the country has been documented in humans. Serotyping studies led to the identification of 36 distinct serotypes, most (73.8%) corresponding to non-clonal variants, with clonal types II and III being rarely detected[62]. Prior work from our group also identified ample variability with molecular resolution in human samples from maternal seroconversion cases[31]. Conspicuously, the genotypes identified in humans cluster partially with those identified in sheep, suggesting that similar, if not the same, strains are present in both species, consistent with the zoonotic potential of toxoplasmosis. These findings underscore the paradigmatic relevance of *T. gondii* to the *One Health* concept whereby environmental, human and animal infections impact both animal and public health.

An inherent limitation of genotyping *T. gondii* from biological samples, be it by RFLP or by other genomic based analyses, is the dependence on the quality of recovered DNA from samples exposed to adverse environmental conditions and the presence of PCR inhibitors in clinical samples. Herein, we failed to amplify and resolve the full extent of genotypic variability; only being able to unequivocally identify 8 distinct genotypes. This number is likely an underestimation which reflects the inherent limitations of conventional typing methods. However, our expanded phylogenetic analysis, which considers SNPs beyond those affecting the restriction patterns considered by RFLP analysis, revealed no further overlap between strains. Our data suggests that the 16 samples might correspond to distinct strains. However, all genotypes remained incompletely characterized as there were typing amplicons we were unable to obtain, precluding us from concluding this unambiguously. The diversity observed in our samples adds to the growing number of epidemiological surveys across diverse regions and host species which have revealed extensive genotypic diversity in *T. gondii*, highlighting a complex population structure with strong geographical signatures. Although hundreds of genetic variants, including numerous non-clonal and non-archetypal strains, have been detected, most human infections in Europe and North America still derive largely from the archetypal type II and III lineages[63]. In contrast, South America, considered the probable center of origin for the species[64], harbors an exceptionally diverse set of lineages. Prior work in Brazil, Colombia, and Argentina has shown that human infections in these countries are predominantly caused by non-clonal, non-archetypal strains[13,51,65–68]. Consistent with this regional complexity, the genotypes identified in our study differ from those previously isolated in Argentina by Pardini and colleagues[68], do not match any of the previously described Brazilian genotypes, and only one genotype matched two previously reported genotypes detected in samples from Central and North America (TgShUru17 with TgCKGa04 and TgSKMs3).

Despite growing recognition of the remarkable genetic diversity of *T. gondii* in South America, the phenotypic consequences of most non-archetypal and recombinant lineages remain largely unknown. Whereas the virulence and pathogenesis of the three clonal types are well-characterized in model systems, the majority of non-clonal and non-archetypal genotypes cannot yet be linked to defined biological features. Herein, we isolated two novel *T. gondii* strains, TgUru1 and TgUru2, which displayed unique non-clonal genotypes consistent with recombinant ancestry. Their phenotypic characterization allowed us to correlate their genotype to relevant physiological properties. Both isolates were recovered from ovine abortion cases, a disease outcome consistent with elevated parasite virulence, yet the isolates exhibited different virulence and growth profiles in mice and cellular culture. TgUru1 showed extreme virulence and rapid intracellular proliferation, whereas TgUru2 displayed moderate virulence but enhanced cystogenic capacity. These contrasting phenotypes among genetically distinct strains illustrate how genetic diversity may influence infection dynamics and potentially the severity of infection when present. We speculate that highly virulent genotypes such as TgUru1 could be associated with acute infections leading to early fetal loss, while less virulent but persistent strains such as TgUru2 might underline late term abortions of subclinical gestational infections, or even underlie vertical transmission in cases of infection reactivation, a phenomenon observed to occur in experimentally infected sheep[69]. However, further work would be required to gauge whether the phenotype observed in the mouse model could be correlated with that in sheep.

Distinct genetic backgrounds of *Toxoplasma gondii* have been associated with varying degrees of disease severity in humans. While some strains exhibit heightened virulence, others, including non-archetypal lineages, have been described as moderately virulent or even avirulent[13,70–73]. There is also evidence suggesting that parasite genetic diversity may influence placental tropism and, consequently, the likelihood of vertical transmission[74]. In addition, lack of cross-strain protection from vertical transmission during reinfection in pregnancy has been experimentally shown in sheep[69] and demonstrated to occur naturally in humans[75]. Together, these observations highlight the potential complexity of host–parasite interactions in the context of congenital infection and suggest that strain diversity could influence transmission dynamics and disease outcome. These considerations may have implications for the design of prophylactic strategies, particularly in regions where parasite diversity is high. In this context, a more comprehensive characterization of parasite diversity, coupled with systematic isolation and experimental analysis of strains, will be important to better define genotype–phenotype relationships and to understand their evolutionary and clinical relevance.

In light of the phenotypic differences observed between our isolates, we examined genomic variation beyond genotyping markers. While overall genome structure remained largely conserved, we identified clear differences in ROP5 copy number between TgUru1 and TgUru2. Phylogenetic classification showed that the copies present in both strains fall within the three canonical subtypes (A, B, and C) described by[57]. Despite the broader diversity reported for the ROP5 family in T. gondii, the copies assigned to each subtype were highly conserved across key functional regions—including the IRGa6-binding interface, the HGR/HGH catalytic triad, and the DVS motif—with the exception of a two-guanine deletion detected in one TgUru1 copy. This conservation is consistent with the essential role of the ROP5 pseudokinase domain in modulating the IRG response and acute virulence[18,76].

Although previous studies have not identified a global correlation between ROP5 copy number and virulence across major *T. gondii* lineages[18,57], more recent work suggests that locus expansion may influence virulence in admixed strains[19]. The isolates analyzed here share similar ROP5 allele types but differ in both virulence and copy number, particularly in ROP5A and ROP5C. In this context, variation in ROP5 dosage may contribute to

differences in virulence, potentially through its role in IRG evasion[77]. Despite high overall sequence identity (~95%), our phylogenetic analysis indicates that the ROP5 repertoire extends beyond the canonical subtypes defined in laboratory strains[57] revealing a continuum of diversity likely shaped by adaptation to different host IRG repertoires[18,57]. Consistent with these observations, whole-genome analyses identified variation in loci previously associated with parasite virulence, including differences in ROP5 copy number. However, our data do not allow us to establish a direct relationship between these genomic features and abortion outcomes in sheep. Rather, these findings suggest that the isolates characterized here possess genomic traits that may contribute to parasite fitness or virulence and highlight the need for further studies addressing their functional relevance in the context of infection and disease.

Our detailed phylogenomic analysis shows that the three Uruguayan isolates (TgUru1, TgUru2 and the previously obtained CASTELLS) fall into distinct clades, consistent with independent evolutionary histories. This pattern mirrors the genomic structure described by Galal et al. (2022), where chromosome-painting ancestry profiles correspond closely to genome-wide phylogenetic relationships[51]. Alongside with previous work showing that South American *T. gondii* populations are highly admixed and often display mosaic genomes shaped by limited recombination, these results underscore the remarkable genetic diversity characteristic of "New World" parasites[51,78]. Notably, despite the much larger number of Brazilian genomes included in our analysis, the breadth of diversity represented by only three Uruguayan isolates is comparable, suggesting that Uruguay harbors a similarly heterogeneous reservoir of *T. gondii* genotypes. The absence of major geographic barriers between Uruguay and Brazil—combined with the documented movement of wildlife and livestock (and people) across the dry border—likely contributes to this shared diversity, a pattern also observed in other zoonotic pathogens such as *Mycobacterium bovis*[79]. A more comprehensive assessment of how geographical barriers influence the regional distribution of *T. gondii* genotypes will require broader genomic sampling, especially of underrepresented regions like Argentina, Paraguay, and Chile.

Overall, this study provides new insight into the diversity of *Toxoplasma gondii* associated with ovine abortion in Uruguay and highlights the presence of genetically distinct strains circulating in sheep. By combining population-level genotyping with experimental and genomic characterization of isolates, our work contributes to a more comprehensive understanding of parasite diversity and biological traits relevant to infection in livestock. Future studies integrating epidemiological, experimental, and genomic data will be important to further elucidate the factors influencing disease outcomes in naturally infected animals.

Data availability

The datasets generated during and/or analyzed during the current study are available in the NCBI's GenBank database, and can be retrieved using the individual identifiers provided in supplementary material.

Received: 13 January 2026; Accepted: 26 May 2026
Published online: 05 June 2026

References

1. Kim, K. & Weiss, L. M. *Toxoplasma gondii*: The model apicomplexan. *Int. J. Parasitol.* **34**, 423–432 (2004).
2. Furtado, J., Smith, J., Belfort, R., Gattey, D. & Winthrop, K. Toxoplasmosis: A global threat. *J. Glob. Infect. Dis.* **3**281. (2011).
3. Weiss, L. M. & Kim, K. The development and biology of bradyzoites of *Toxoplasma gondii*. *Front. Biosci.* https://doi.org/10.2741/Weiss (2000).
4. Dubey, J. P. & Frenkel, J. K. Cyst-induced toxoplasmosis in cats. *J. Protozool.* **19**, 155–177 (1972).
5. Dubey, J. P., Miller, N. L. & Frenkel, J. K. The *Toxoplasma gondii* oocyst from cat feces. *J. Exp. Med.* **132**, 636–662 (1970).
6. Frenkel, J. K. Toxoplasma in and around us. *Bioscience* **23**, 343–352 (1973).
7. Wolf, A., Cowen, D. & Paige, B. Human Toxoplasmosis: Occurrence in Infants as an Encephalomyelitis Verification by Transmission to Animals. *Sci. (80-).* **89**, 226–227 (1939).
8. U., A. H. M. M. Review on diagnosis and molecular characterization of *Toxoplasma gondii* in humans and animals. *Trop. Biomed.* **38**, 511–539 (2021).
9. Ajzenberg, D. et al. Genetic diversity, clonality and sexuality in *Toxoplasma gondii*. *Int. J. Parasitol.* **34**, 1185–1196 (2004).
10. Howe, D. K. & Sibley, L. D. *Toxoplasma gondii* comprises three clonal lineages: Correlation of parasite genotype with human disease. *J. Infect. Dis.* **172**, 1561–1566 (1995).
11. Dini, F. M. et al. Multiple Typing Approach to Characterize Toxoplasma gondii Strains from Captive and Livestock Species in Northern Italy Suggests the Circulation of Type-II Variants. *Animals* **14**, 3597 (2024).
12. Fernández-Escobar, M. et al. Isolation and genetic characterization of *Toxoplasma gondii* in Spanish sheep flocks. *Parasit. Vectors.* **13**, 396 (2020).
13. de Lima Bessa, G., de Almeida Vitor, R. W. & dos Santos Martins-Duarte, E. *Toxoplasma gondii* in South America: A differentiated pattern of spread, population structure and clinical manifestations. *Parasitol. Res.* **120**, 3065–3076 (2021).
14. de Lima Bessa, G. et al. In vitro and in vivo susceptibility to sulfadiazine and pyrimethamine of *Toxoplasma gondii* strains isolated from Brazilian free wild birds. *Sci. Rep.* **13**, 7359 (2023).
15. Rajendran, C., Su, C. & Dubey, J. P. Molecular genotyping of Toxoplasma gondii from Central and South America revealed high diversity within and between populations. *Infect. Genet. Evol.* **12**, 359–368 (2012).
16. Su, C., Shwab, E. K., Zhou, P., Zhu, X. Q. & Dubey, J. P. Moving towards an integrated approach to molecular detection and identification of *Toxoplasma gondii*. *Parasitology* **137**, 1–11 (2010).
17. Calero-Bernal, R., Fernández-Escobar, M., Katzer, F., Su, C. & Ortega-Mora, L. M. Unifying virulence evaluation in *Toxoplasma gondii*: A timely task. *Front. Cell. Infect. Microbiol.* **12**, 868727 (2022).
18. Behnke, M. S. et al. Rhoptry proteins ROP5 and ROP18 are major murine virulence factors in genetically divergent South American strains of *Toxoplasma gondii*. *PLoS. Genet.* https://doi.org/10.1371/journal.pgen.1005434 (2015).
19. Xia, J. et al. Third-generation sequencing revises the molecular karyotype for *Toxoplasma gondii* and identifies emerging copy number variants in sexual recombinants. *Genome. Res.* **31**, 834–851 (2021).
20. Dorsch, M. A. et al. Diagnostic Investigation of 100 Cases of Abortion in Sheep in Uruguay: 2015–2021. *Front Vet. Sci.* **9**, 904786 (2022).
21. Freyre, A. et al. Aborto ovino toxoplásmico en un establecimiento de Florida. *Vet* **29**, 5–9 (1994).

22. Freyre, A. et al. The incidence and economic significance of ovine toxoplasmosis in Uruguay. *Veterinary Parasitology* at (1999). https://doi.org/10.1016/S0304-4017(98)00215-5
23. Freyre, A., Perdomo, E., Bonino, J. & Falcon, J. D. Aborto ovino toxoplásmico: Su comprobación en el Uruguay. *Vet* **23**, 6–12 (1987).
24. Dorsch, M. A. et al. Bacterial, protozoal and viral abortions in sheep and goats in South America: A review. *Small. Rumin. Res.* **205**, 106547 (2021).
25. Freyre, A. et al. The incidence and economic significance of ovine toxoplasmosis in Uruguay. *Vet. Parasitol.* **73**, 13–15 (1997).
26. Jensen, K. D. C. et al. *Toxoplasma gondii* superinfection and virulence during secondary infection correlate with the exact ROP5/ROP18 allelic combination. *MBio* https://doi.org/10.1128/mBio.02280-14 (2015).
27. Schares, G., Vrhovec, M. G., Pantchev, N., Herrmann, D. C. & Conraths, F. J. Occurrence of Toxoplasma gondii and Hammondia hammondi oocysts in the faeces of cats from Germany and other European countries. *Vet. Parasitol.* **152**, 34–45 (2008).
28. Reischl, U., Bretagne, S., Krüger, D., Ernault, P. & Costa, J. M. Comparison of two DNA targets for the diagnosis of Toxoplasmosis by real-time PCR using fluorescence resonance energy transfer hybridization probes. *BMC Infect. Dis.* **3**, 7 (2003).
29. Su, C., Zhang, X. & Dubey, J. P. Genotyping of Toxoplasma gondii by multilocus PCR-RFLP markers: A high resolution and simple method for identification of parasites. *Int. J. Parasitol.* **36**, 841–848 (2006).
30. Castro, B. B. P., Gennari, S. M., Lorenzi, H. & Su, C. A simple method to generate PCR-RFLP typing profiles from DNA sequences in Toxoplasma gondii. *Infect. Genet. Evol.* **85**, 104590 (2020).
31. Valentin-Decuadro, A. et al. Toxoplasma gondii seroprevalence, seroconversion rates and genetic variability in humans from Uruguay. *Parasitology* **152**, 860–870 (2025).
32. Katoh, K. MAFFT: a novel method for rapid multiple sequence alignment based on fast Fourier transform. *Nucleic Acids Res.* **30**, 3059–3066 (2002).
33. Krah, F. S. & Heibl, C. rGUIDANCE – alignment confidence score computation in R. *J. Open. Source Softw.* **4**, 1350 (2019).
34. Stamatakis, A. RAxML version 8: a tool for phylogenetic analysis and post-analysis of large phylogenies. *Bioinformatics* **30**, 1312–1313 (2014).
35. Cabrera, A. et al. Isolation and molecular characterization of four novel *Neospora caninum* strains. *Parasitol. Res.* https://doi.org/10.1007/s00436-019-06474-9 (2019).
36. Cabrera, A. et al. New insights into phenotype and genotype relationships in Neospora caninum. *Front Vet. Sci.* **10**, 1214971. (2023).
37. Francia, M. E. et al. A homolog of structural maintenance of chromosome 1 is a persistent centromeric protein which associates with nuclear pore components in *Toxoplasma gondii*. *Front. Cell. Infect. Microbiol.* https://doi.org/10.3389/fcimb.2020.00295 (2020).
38. Cervantes, P. W., Martorelli Di Genova, B., Erazo Flores, B. J. & Knoll, L. J. RIPK3 facilitates host resistance to oral *Toxoplasma gondii* infection. *Infect. Immun.* https://doi.org/10.1128/IAI.00021-21 (2021).
39. Koren, S. et al. Canu: scalable and accurate long-read assembly via adaptive k-mer weighting and repeat separation. *bioRxiv* (2016). https://doi.org/10.1101/071282 doi:10.1101/071282.
40. Walker, B. J. et al. Pilon: An integrated tool for comprehensive microbial variant detection and genome assembly improvement. *PLoS One* https://doi.org/10.1371/journal.pone.0112963 (2014).
41. Li, H. Aligning sequence reads, clone sequences and assembly contigs with BWA-MEM. arXiv:1303.3997 https://doi.org/10.48550/arXiv.1303.3997 (2013) .
42. Assefa, S., Keane, T. M., Otto, T. D., Newbold, C. & Berriman, M. ABACAS: Algorithm-based automatic contiguation of assembled sequences. *Bioinformatics* **25**, 1968–1969 (2009).
43. Kim, D., Langmead, B. & Salzberg, S. L. HISAT: A fast spliced aligner with low memory requirements. *Nat. Methods.* https://doi.org/10.1038/nmeth.3317 (2015).
44. Kim, D., Paggi, J. M., Park, C., Bennett, C. & Salzberg, S. L. Graph-based genome alignment and genotyping with HISAT2 and HISAT-genotype. *Nat. Biotechnol.* **37**, 907–915 (2019).
45. Pertea, M., Kim, D., Pertea, G. M., Leek, J. T. & Salzberg, S. L. Transcript-level expression analysis of RNA-seq experiments with HISAT, StringTie and Ballgown. *Nat. Protoc.* https://doi.org/10.1038/nprot.2016.095 (2016).
46. Steinbiss, S. et al. Companion: A web server for annotation and analysis of parasite genomes. *Nucleic Acids Res.* https://doi.org/10.1093/nar/gkw292 (2016).
47. Delcher, A. L., Salzberg, S. L. & Phillippy, A. M. Using MUMmer to Identify Similar Regions in Large Sequence Sets. *Curr Protoc. Bioinforma* Feb 10: Unit 10.3 https://doi.org/10.1002/0471250953.bi1003s00 (2003).
48. Nattestad, M. & Schatz, M. C. Assemblytics: A web analytics tool for the detection of variants from an assembly. *Bioinformatics* https://doi.org/10.1093/bioinformatics/btw369 (2016).
49. Krzywinski, M. et al. Circos: An information aesthetic for comparative genomics. *Genome Res.* (9), https://doi.org/10.1101/gr.092759.109 (2009).
50. Minh, B. Q. et al. IQ-TREE 2: New models and efficient methods for phylogenetic inference in the genomic era. *Mol. Biol. Evol.* **37**, 1530–1534 (2020).
51. Galal, L. et al. A unique *Toxoplasma gondii* haplotype accompanied the global expansion of cats. *Nat. Commun.* **13**, 5778 (2022).
52. Berná, L. et al. Reevaluation of the Toxoplasma gondii and Neospora caninum genomes reveals misassembly, karyotype differences, and chromosomal rearrangements. *Genome Res.* **31**, 823–833 (2021).
53. McKenna, A. et al. The Genome Analysis Toolkit: A MapReduce framework for analyzing next-generation DNA sequencing data. *Genome Res.* **20**, 1297–1303 (2010).
54. Letunic, I. & Bork, P. Interactive Tree Of Life (iTOL) v5: an online tool for phylogenetic tree display and annotation. *Nucleic Acids Res.* **49**, W293–W296 (2021).
55. Percie du Sert. The ARRIVE guidelines 2.0: Updated guidelines for reporting animal research. *PLOS Biol.* **18**, e3000410 (2020).
56. Singh, S. et al. *Toxoplasma gondii* virulence in mice is determined by the pseudokinase ROP5B and countered by an IRG-GBP protein interplay. *Front. Immunol.* https://doi.org/10.3389/fimmu.2025.1593785 (2025).
57. Reese, M. L., Zeiner, G. M., Saeij, J. P. J., Boothroyd, J. C. & Boyle, J. P. Polymorphic family of injected pseudokinases is paramount in *Toxoplasma* virulence. *Proc. Natl. Acad. Sci. U. S. A.* 9625–30 (2011).
58. Vos, T. et al. Global burden of 369 diseases and injuries in 204 countries and territories, 1990–2019: a systematic analysis for the Global Burden of Disease Study 2019. *Lancet* **396**, 1204–1222 (2020).
59. Hajimohammadi, B. et al. A Meta-Analysis of the Prevalence of Toxoplasmosis in Livestock and Poultry Worldwide. *Ecohealth* **19**, 55–74 (2022).
60. Hill, D. E. & Dubey, J. P. Toxoplasma gondii. In *Foodborne Parasites* 119–138 (Springer International Publishing, 2018). https://doi.org/10.1007/978-3-319-67664-7_6.
61. Innes, E. A., Bartley, P. M., Buxton, D. & Katzer, F. Ovine toxoplasmosis. *Parasitology* **136**, 1887–1894 (2009).
62. Sousa, S., Puime, A., Costa, J. M. C. & Dardé, M. L. da Serotyping Toxoplasma Gondii: A Cross-Sectional Study in Uruguay. *J. Infect. Dis. Epidemiol.* 3, (2017).
63. Hosseini, S. A. et al. Human toxoplasmosis: a systematic review for genetic diversity of Toxoplasma gondii in clinical samples. *Epidemiol. Infect.* **147**, e36 (2019).
64. Cañón-Franco, W., López-Orozco, N., Gómez-Marín, J. & Dubey, J. P. An overview of seventy years of research (1944–2014) on toxoplasmosis in Colombia, South America. *Parasit. Vectors.* **7**, 427 (2014).

65. Ajzenberg, D., Bañuls, A. L., Tibayrenc, M. & Dardé, M. L. Microsatellite analysis of Toxoplasma gondii shows considerable polymorphism structured into two main clonal groups. *Int. J. Parasitol.* **32**, 27–38 (2002).
66. Ferreira, I. M. R. et al. *Toxoplasma gondii* isolates: Multilocus RFLP–PCR genotyping from human patients in Sao Paulo State, Brazil identified distinct genotypes. *Exp. Parasitol.* 190–195 (2011).
67. Pardini, L. et al. First isolation and molecular characterization of *Toxoplasma gondii* from a human placenta in Argentina. *Parasitol. Int.* (2), https://doi.org/10.1016/j.parint.2013.10.011 (2014).
68. Pardini, L. et al. Congenital human toxoplasmosis caused by non-clonal *Toxoplasma gondii* genotypes in Argentina. *Parasitol. Int.* 48–52 (2019).
69. Chiebao, D. P. et al. Congenital transmission of *Toxoplasma gondii* after experimental reinfection with Brazilian typical strains in chronically infected sheep. *Front. Vet. Sci.* https://doi.org/10.3389/fvets.2019.00093 (2019).
70. Sanchez, S. G. & Besteiro, S. The pathogenicity and virulence of Toxoplasma gondii. *Virulence* **12**, 3095–3114 (2021).
71. Brito, R. et al. Genetic diversity of *Toxoplasma gondii* in South America: Occurrence, immunity, and fate of infection. *Parasit. Vectors* 461. (2023).
72. Benavides, J. et al. Development of lesions and tissue distribution of parasite in lambs orally infected with sporulated oocysts of *Toxoplasma gondii*. *Vet. Parasitol.* **179**, 209–215 (2011).
73. Rico-Torres, C. P., Vargas-Villavicencio, J. A. & Correa, D. Is Toxoplasma gondii type related to clinical outcome in human congenital infection? Systematic and critical review. *Eur. J. Clin. Microbiol. Infect. Dis.* **35**, 1079–1088 (2016).
74. Arranz-Solís, D., Mukhopadhyay, D. & Saeij, J. J. P. *Toxoplasma* effectors that affect pregnancy outcome. *Trends Parasitol.* **37**, 283–295. https://doi.org/10.1016/j.pt.2020.10.013 (2021).
75. Elbez-Rubinstein, A. et al. Congenital toxoplasmosis and reinfection during pregnancy: Case report, strain characterization, experimental model of reinfection, and review. *J. Infect. Dis.* **199**, 280–285 (2009).
76. Behnke, M. S. et al. Virulence differences in *Toxoplasma* mediated by amplification of a family of polymorphic pseudokinases. *Proceedings of the National Academy of Sciences* 9631–9636 (2011).
77. Niedelman, W. et al. The rhoptry proteins ROP18 and ROP5 mediate *Toxoplasma gondii* evasion of the murine, but not the human, Interferon-Gamma response. *PLoS Pathog.* **8**, e1002784 (2012).
78. Lorenzi, H. et al. Local admixture of amplified and diversified secreted pathogenesis determinants shapes mosaic Toxoplasma gondii genomes. *Nat. Commun.* **7**, 10147 (2016).
79. Lasserre, M. et al. Whole genome sequencing of the monomorphic pathogen *Mycobacterium bovis* reveals local differentiation of cattle clinical isolates. *BMC Genomics* https://doi.org/10.1186/s12864-017-4249-6 (2018).

Acknowledgements

LRT was a doctoral student of PEDECIBA-Biología. LB, PF, FG, MEF are researchers of PEDECIBA and the national system of researchers (SNI-ANII). We are deeply thankful for the everlasting contributions of Dr. Alvaro Freyre, and Dr. Dario Falcon, to the Toxoplasma research in Uruguay upon which we have built on in this manuscript.

Author contributions

L.T.-H. contributed to methodology, investigation, data curation, formal analysis, and writing – original draft. P.F., A.M.C., and A.V. contributed to methodology and investigation, with P.F. also contributing to formal analysis. M.D. and S.F. provided resources. F.G. contributed to conceptualization and resources. L.B. and M.E.F. contributed to conceptualization, investigation, data curation, formal analysis, writing – review & editing, and supervision. M.E.F. additionally contributed to project administration and funding acquisition. All authors read and approved the final manuscript.

Funding

This project was funded by the National Agency for Research and Innovation (grant FSSA_1_2019_1_159912 awarded to MEF). The IPM is funded by FOCEM - Fondo para la Convergencia Estructural del Mercosur (Grant COF 03/11). LRT was funded by a doctoral fellowship from ANII (POS_FSSA_2020_1_1010115). Sampling of aborted sheep was partially funded by grants FCE_3_2018_1_148540 from ANII to FG and SF, and PL_27 from INIA.

Declarations

Competing interests

The authors declare no competing interests.

Additional information

Supplementary Information The online version contains supplementary material available at https://doi.org/10.1038/s41598-026-55698-0.

Correspondence and requests for materials should be addressed to L.B. or M.E.F.